Am J Cancer Res 2024;14(5):2103-2123
www.ajcr.us /ISSN:2156-6976/ajcr0155746

Original Article

The lncRNA TPT1-AS1 promotes the survival of neuroendocrine prostate cancer cells by facilitating autophagy

Po-An Chen[1*], Pei-Ching Chang[1,2*], Wayne W Yeh[1,3], Tze-Yun Hu[1], Yung-Chih Hong[4], Yu-Chao Wang[5], William J Huang[6,7], Tzu-Ping Lin[6,7]

[1]Institute of Microbiology and Immunology, National Yang Ming Chiao Tung University, Hsinchu 30010, Taiwan; [2]Cancer Progression Research Center, National Yang Ming Chiao Tung University, Taipei 11221, Taiwan; [3]Section of Infection and Immunity, Herman Ostrow School of Dentistry, Norris Comprehensive Cancer Center, University of Southern California, Los Angeles, CA 90089, USA; [4]Faculty of Medicine, National Yang Ming Chiao Tung University, Hsinchu 30010, Taiwan; [5]Institute of Biomedical Informatics, National Yang Ming Chiao Tung University, Hsinchu 30010, Taiwan; [6]Department of Urology, Taipei Veterans General Hospital, Taipei 11217, Taiwan; [7]Department of Urology, School of Medicine and Shu-Tien Urological Research Center, National Yang Ming Chiao Tung University, Hsinchu 30010, Taiwan. [*]Co-first authors.

Received February 2, 2024; Accepted April 21, 2024; Epub May 15, 2024; Published May 30, 2024

Abstract: The lncRNA tumor protein translationally controlled 1-antisense RNA 1 (TPT1-AS1) is known for its oncogenic role in various cancers, but its impact on the pathological progression of prostate cancer remains unclear. Our previous study demonstrated that the RE1-silencing transcription factor (REST) regulates neuroendocrine differentiation (NED) in prostate cancer (PCA) by derepressing specific long non-coding RNAs (lncRNAs), including TPT1-AS1. In this study, we revealed that TPT1-AS1 is overexpressed in LNCaP and C4-2B cells after IL-6 and enzalutamide treatment. By analyzing The Cancer Genome Atlas (TCGA) prostate adenocarcinoma dataset, we detected upregulated TPT1-AS1 expression in neuroendocrine-associated PCA but not in prostate adenocarcinoma. Single-cell RNA sequencing data further confirmed the increased TPT1-AS1 levels in neuroendocrine prostate cancer (NEPC) cells. Surprisingly, functional experiments indicated that TPT1-AS1 overexpression had no stimulatory effect on NED in LNCaP cells and that TPT1-AS1 knockdown did not inhibit IL-6-induced NED. Transcriptomic analysis revealed the essential role of TPT1-AS1 in synaptogenesis and autophagy activation in neuroendocrine differentiated PCA cells induced by IL-6 and enzalutamide treatment. TPT1-AS1 was found to regulate the expression of autophagy-related genes that maintain neuroendocrine cell survival through autophagy activation. In conclusion, our data expand the current knowledge of REST-repressed lncRNAs in NED in PCA and highlight the contribution of TPT1-AS1 to protect neuroendocrine cells from cell death rather than inducing NED. Our study suggested that TPT1-AS1 plays a cytoprotective role in NEPC cells; thus, targeting TPT1-AS1 is a potential therapeutic strategy.

Keywords: Prostate cancer, neuroendocrine prostate cancer (NEPC), long non-protein coding RNA (LncRNA)

Introduction

Persistent exposure to second-generation androgen receptor inhibitors (ARIs) leads to the development of treatment-induced neuroendocrine prostate cancer (NEPC) [1, 2], a highly aggressive subtype of castration-resistant prostate cancer (CRPC) [3]. NEPC is distinguished by an epithelial lineage switch from an androgen receptor (AR)-positive to a neuroendocrine-positive state, resulting in the acquisition of AR independence [4]. This transition makes NEPC a major contributor to the resistance of CRPC to new-generation ARIs, including enzalutamide [5, 6]. Therefore, while new-generation ARIs provide initial therapeutic advantages [7, 8], prolonged use may ultimately lead to the emergence of a more challenging-to-treat manifestation, specifically NEPC. Furthermore, neuroendocrine tumors actively secrete various signaling molecules, establishing paracrine communication within the tumor microenvironment and promoting tumor progression [9]. A comprehensive understanding

https://doi.org/10.62347/IMBV8599

of the molecular mechanisms underlying NEPC is needed for developing new treatments for prostate cancer (PCA) to prevent the emergence of more challenging-to-treat manifestations after prolonged use of ARIs.

The epithelial lineage of castration-resistant prostate adenocarcinoma that switches to a neuroendocrine lineage carcinoma has been studied by both genomic and molecular approaches [10-12]. The main characteristics involved in the epigenetic regulation of this transdifferentiation include the gain of MYCN and its stabilizing factor Aurora A kinase (AURKA) [13-15] and the loss of RE1-silencing transcription factor (REST) [16-19]. REST, also known as neuron restrictive silencing factor (NRSF), is well known for its ability to assemble repressive epigenetic complexes to silence neuronal differentiation genes in neural progenitor and non-neuronal cells [20]. The repressive role of REST in regulating the neuroendocrine transdifferentiation of PCA cells was first reported in 2014 [16, 17], demonstrating that AR interacts directly with REST, recruits it to the promoters of neuroendocrine lineage genes, and inhibits their expression. Androgen deprivation [17], interleukin-6 (IL-6) [16], and hypoxia [18, 21] have all been shown to induce REST degradation and, consequently, the activation of neuroendocrine transdifferentiation in PCA cells. Mechanistically, REST induces neuroendocrine differentiation (NED) of PCA through the derepression of proteins, such as MAOA [19] and BAF53B [22], as well as long non-coding RNAs (lncRNAs), including HOTAIR [23] and LINC01801 [24]. Notably, loss of REST induced NED in PCA cells is partly linked to the activation of autophagy [16, 18, 19, 23, 24].

Autophagy is a lysosome-mediated degradation pathway that maintains cellular homeostasis and survival by recycling unwanted cytosolic components and damaged organelles [25]. Postmitotic cells, particularly neurons, are highly dependent on autophagy due to their postmitotic nature, making them highly sensitive to toxic proteins and damaged organelles. Moreover, specialized intracellular vesicle trafficking during autophagy is required for efficient cargo recycling in neurons [26, 27]. Thus, autophagy is crucial for maintaining the health of neurons [28]. The role of autophagy in NEPC was initially elucidated by concomitant activation of NED with autophagy in response to various neuroendocrine induction signals, including androgen deprivation, hypoxia, and IL-6 [16, 18, 29]. Consistent with its commitment to control neural fate, REST has also been identified as the key repressor of neuroendocrine differentiated PCA cells induced by androgen deprivation, hypoxia, and IL-6 [16-18]. Notably, the concomitant down-regulation of REST induces NED and autophagy [16, 18]. Mechanistically, a reduction in REST may induce autophagy through the de-repression of autophagy-related genes, such as Atg5 and LC3 [16] or the mitophagy-regulating gene MAOA [19].

LncRNAs are RNA transcripts longer than 200 nucleotides [30, 31] that modulate biological functions by serving as either scaffolds to recruit transcription factors to specific genomic loci [32, 33] or decoys to sequester chromatin-binding proteins or miRNAs [34]. As members of a newly defined novel epigenetic layer for transcriptional regulation, lncRNAs are involved in cancer progression and can act as tumor suppressors and oncogenes [35]. However, their involvement in NEPC remains in its early stages of exploration. To identify REST-regulated lncRNAs that participate in NED in PCA cells, we performed a comprehensive analysis involving transcriptome and small interfering RNA (siRNA) knockdown screening under REST overexpression and knockdown conditions and revealed HOTAIR [23] and LINC01801 [24] as novel NEPC-related lncRNAs implicated in the neuroendocrine differentiation of PCA cells. These data also suggest that lncRNAs may be exploited as novel biomarkers and therapeutic targets for NEPC.

Tumor protein translationally controlled 1-antisense RNA 1 (TPT1-AS1), located at chromosome region 13q14.13 of the TPT1 gene, was initially characterized as an oncogenic [36] and a poor prognosis-related [37] lncRNA in ovarian cancer. Overexpression of TPT1-AS1 was also found to promote the progression of colorectal cancer [38, 39], pancreatic cancer [40], gastric cancer [41], esophageal squamous cell carcinomas [42], and glioblastoma [43]. Conversely, TPT1-AS1 was down-regulated in breast cancer and predicted a poor progno-

sis for breast cancer patients [44, 45]. Furthermore, TPT1-AS1 may have opposite effects on hepatocellular carcinoma cells [46, 47]. Most importantly, its association with PCA remains to be explored.

In this study, we aimed to investigate the role of TPT1-AS1, a REST-repressed lncRNA, in the progression of NEPC. Initially, we confirmed the up-regulation of TPT1-AS1 under neuroendocrine induction conditions and in neuroendocrine-associated PCA, suggesting its potential involvement in the development of NEPC. Surprisingly, neither overexpression nor knockdown experiments targeting TPT1-AS1 affected NED. Transcriptome analysis revealed that TPT1-AS1 activates autophagy, a crucial process known to mediate NED in PCA cells. Interestingly, autophagy activation facilitated by TPT1-AS1 appears to enhance the survival of neuroendocrine cells rather than induce NED. In conclusion, given that the activation of autophagy by TPT1-AS1 is crucial for maintaining the survival of neuroendocrine cells, targeting TPT1-AS1 could induce the death of NEPC cells, thus restoring the efficacy of androgen receptor inhibitors (ARIs).

Materials and methods

Cell culture

LNCaP and C4-2B cells were cultured in RPMI 1640 (Gibco, 31800-014) supplemented with 10% FBS (HyClone, SH30071.03), 1% penicillin/streptomycin, and 30 mg/ml L-glutamine (Sigma-Aldrich, G8540). LNCaP-TR cells were cultured as described for LNCaP cells supplemented with 5 μg/ml blasticidin S (InvivoGen, ant-bl-1). For the generation of TPT1-AS1-inducible LNCaP cell line, TPT1-AS1 cDNA (synthesized by GeneArt, Thermo Fisher Scientific) was cloned and inserted into the pLenti4-CMV/TO vector and introduced into LNCaP-TR cells through lentiviral transduction, followed by selection with 200 μg/ml zeocin (InvivoGen, ant-zn-1). LNCaP-TR-shREST [16] and LNCaP-TR-TPT1-AS1 cells were maintained as described for LNCaP-TR cells supplemented with 50 μg/ml zeocin. All cells were cultured at 37°C in a humidified incubator with 5% CO_2. For drug treatment, LNCaP and C4-2B cells were treated with 100 ng/ml IL-6 in phenol red-free RPMI 1640 (Gibco) supplemented with 10% charcoal/dextran-treated FBS (CDT; HyClone, SH-30068.03) and 50 nM enzalutamide.

siRNA transfection

LNCaP and C4-2B cells were seeded in culture medium at $2×10^5$ cells/well in 6-well plates and transfected with TPT1-AS1 siRNA SMART-Pool (Dharmacon, R-188212-00) at a final concentration of 20 nM using Lipofectamine RNAiMAX (Invitrogen, 13778-150) following the manufacturer's protocol. The sequences used for siRNA-mediated knockdown of TPT1-AS1 were 5'-GCAUAUUAGCAGAUCCAUA-3', 5'-CGGCCAAGUUUUAUGUUAU-3', 5'-CUAAAAUAG-AGCUCUCAAA-3', and 5'-UCCAGUAAAUCCCAA-GCAA-3'. The control siRNA siGLO Green Transfection Indicator (Dharmacon, D-001630-01) was used as a negative control to ensure transfection efficiency.

Real-time reverse transcription and quantitative PCR (real-time RT-qPCR)

Total cell RNA was isolated by TRIzol (Invitrogen, 15596-018). To detect mRNAs and lncRNAs, cDNA was generated with a SuperScript™ III First-Strand Synthesis System Kit (Invitrogen, 18080-085) using Oligo-(dT). Both RNA extraction and cDNA synthesis were performed following the manufacturer's procedures. Real-time qPCR analysis was carried out in 96-well plates with Bio-Rad CFX96 real-time PCR detection system. All expression levels were normalized against GAPDH. The pairs of qPCR primers used were designed with PerlPrimer (http://perlprimer.sourceforge.net/). The primer sequences are listed in Table S1.

High-throughput RNA sequencing (RNA-seq) and Gene Ontology (GO) data analysis

Total RNA was extracted from control and TPT1-AS1 knockdown LNCaP cells treated with or without 100 ng/ml IL-6 in phenol red-free RPMI 1640 (Gibco, 31800022) supplemented with 10% charcoal/dextran-treated FBS (CDT; HyClone, SH30068.03) and from LNCaP cells treated with or without 50 nM enzalutamide. RNA-seq was performed using the Illumina NextSeq 2000 platform (Illumina, Inc., San Diego, CA, USA), and the raw reads were aligned to human reference genome GRCh38/hg38. Partek Flow (Partek, version 11.0.24.0102)

was used to calculate the abundances of the transcripts. Transcriptome information was obtained from RefSeq transcripts. To identify biological functions, the differentially expressed mRNAs were subjected to canonical pathway analysis using Ingenuity Pathway Analysis software (http://www.ingenuity.com).

Immunoblotting

Cells were lysed in NP-40 lysis buffer (0.5% NP-40 (Amresco, E109)), 1× PBS and 1× protease inhibitor (Roche, 04693132001) or RIPA lysis buffer (50 mM Tris, pH 7.4; 150 mM NaCl; 1% NP-40; 1% sodium deoxycholate; 1 mM EDTA; ddH_2O). The protein concentrations were measured using Bio-Rad protein assay dye reagent (Bio-Rad, 500-0006) according to the manufacturer's protocol. Protein samples were resolved by SDS-polyacrylamide gel electrophoresis (SDS-PAGE), transferred to 0.2 μm pore size PVDF membranes by Trans-Blot Turbo RTA Transfer System (Bio-Rad, 704272), blocked with 5% BSA in 1× TBST or 5% skim milk in 1× TBST, immunoblotted with primary antibodies against each of the indicated proteins, incubated with horseradish peroxidase (HRP)-conjugated secondary antibodies, visualized with Pierce ECL Western Blotting Substrate (Thermo Scientific, 34080) and imaged using a Luminescence/Fluorescence Imaging System (FUJIFILM, LAS-4000). The primary antibodies used were anti-REST (Millipore, 07-579), anti-AR (Millipore, 06-680), anti-TUBIII (Sigma Aldrich, T2200), anti-CHGA (Thermo Fisher Scientific, MA5-13096), anti-NSE (Cell Signaling, 9536), anti-SYP (GeneTex, GTX100-865), anti-LC3 (Cell Signaling, 2775S), and anti-GAPDH (GTX100118).

Cell proliferation assay

LNCaP and C4-2B cells were seeded in 96-well plates, transfected with either siRNA targeting TPT1-AS1 (siTPT1-AS1) or siGLO for 48 hours, and then treated with 100 ng/mL IL-6 in phenol red-free RPMI-1640 supplemented with 10% CDT or 50 nM enzalutamide for 72 hours. After treatment, 3-(4,5-dimethylthiazol-2-yl)-2,5-diphenyltetrazolium bromide (MTT) assay was performed according to the manufacturer's instructions. The absorbance (570 and 660 nm) was measured using a TECAN 200Pro (Tecan, Germany) multimode microplate reader. The same volume of medium was used as a blank control.

Neurite outgrowth assay

LNCaP cells were seeded on coverslips in 6 well plates at a density of $1×10^5$ cell/well. Following the indicated treatments, the cells were washed twice with PBS, fixed with 4% paraformaldehyde/PBS for 20 minutes at room temperature, washed twice with PBS, and stained with Cell Membrane Stain (Invitrogen, A15001) according to the manufacturer's instructions. Finally, the coverslips were stained with Hoechst 33342 (Invitrogen, H35770) for 5 minutes at room temperature, mounted in mounting solution (Dako, S30-23), visualized/photographed by fluorescence microscopy (Lecia, DMI4000B), and analyzed using MetaMorph (Molecular Devices, Neurite Outgrowth).

miRNA target prediction

DIANA-TarBase-v9.0 (https://dianalab.e-ce.uth.gr/tarbasev9) was used to predict the miRNAs that interacted with mRNAs.

The Cancer Genome Atlas (TCGA) database

RNA-seq profiles of clinical data from 33 different cancers were downloaded from TCGA. TPT1-AS1 expression was analyzed in 23 cancer tissues that contained corresponding normal tissues using two-tailed Student's t-test.

Single-cell data processing and cell-type annotation

The raw sequencing data were processed using the Cell Ranger (10× Genomics, version 3.1.0) analysis pipeline, followed by alignment to the human reference genome (GRCh38). The high-quality cells included were adapted from the original article for further analysis using Partek Flow (Partek, version 11.0.24.0102). Gene counts were normalized by log2(CPM+1), and genes that were not expressed in more than 99.9% of cells were excluded. Cells were clustered by graph-based clustering and visualized by t-distributed stochastic neighbor embedding (t-SNE). Luminal cells were identified based on the expression of EPCAM and keratin 8 (KRT8). Biomarker genes were identified using the compute biomarkers function in

Partek Flow, and genes with a fold change ≥2 and a *p*-value <0.05 were selected. Biomarker genes were subjected to GO analysis using ingenuity pathway analysis (IPA) software (QIAGEN).

Statistical analysis

Statistical analysis was performed using *Student's-t* test. The data are indicated as *P<0.05; **P<0.01; ***P<0.001. Statistically nonsignificant data are not shown.

Results

TPT1-AS1 increases in prostate adenocarcinoma cells undergoing neuroendocrine differentiation (NED)

To identify NEPC-associated lncRNAs, we combined REST knockdown transcriptomic analysis with siRNA screening and identified 14 potential lncRNAs, including TPT1-AS1 [24]. The RNA-seq data revealed that TPT1-AS1 expression increased following REST knockdown for 3 and 6 days (**Figure 1A**, left panel) [18], and this increase was validated by RT-qPCR (**Figure 1A**, right panel). Subsequently, we analyzed the expression of TPT1-AS1 under NED induction conditions, which coincided with a reduction in REST levels, including treatment with IL-6 and the androgen receptor antagonist enzalutamide (**Figure 1B** and **1C**, left panel). RNA-seq data demonstrated that TPT1-AS1 was up-regulated after IL-6 treatment for 24 to 48 hours but not after 12 hours (**Figure 1D**). The increase in TPT1-AS1 expression following IL-6 and enzalutamide treatment for 72 hours was further confirmed by RT-qPCR analysis (**Figure 1B** and **1C**, right panel).

To investigate whether TPT1-AS1 is a direct target of REST, we examined the promoter region of TPT1-AS1 (transcription start site (TSS) to ±1,000 bp) for possible REST binding sites (RE-1) using JASPAR (http://jaspar.genereg.net/). Unexpectedly, no RE-1 sites were identified within this region. However, it is plausible that REST might bind to genomic sequences through non-canonical RE-1 sites. Thus, we checked our ChIP-seq data published in 2018 to identify potential REST-binding sites [23]. Unfortunately, the data consistently revealed no evidence of REST binding to the TPT1-AS1 promoter. Thus, up-regulation of TPT1-AS1 in NEPC cells may be independent of direct REST repression, suggesting potential alternative regulatory mechanisms that warrant future study.

Expression profiles of TPT1-AS1 in human cancers

TPT1-AS1 has been found to be dysregulated in various cancers, and its expression is associated with patient prognosis. Notably, elevated TPT1-AS1 expression has been linked to poor prognosis in ovarian cancer [37], colorectal cancer [38, 39], pancreatic cancer [40], gastric cancer [41], and hepatocellular carcinoma [47]. Conversely, lower expression of TPT1-AS1 has been correlated with unfavorable outcomes in patients with breast cancer [44, 45]. To summarize the dysregulation of TPT1-AS1 in cancers, we analyzed the expression of TPT1-AS1 in clinical samples from the TCGA database. We discovered significant increases in TPT1-AS1 expression in colon adenocarcinoma (COAD), cholangiocarcinoma (CHOL), head and neck squamous cell carcinoma (HNSC), kidney renal clear cell carcinoma (KIRC), kidney renal papillary cell carcinoma (KIRP), liver hepatocellular carcinoma (LIHC), and rectum adenocarcinoma (READ) (**Figure 2A**). Conversely, TPT1-AS1 exhibited decreased expression in breast cancer (BRCA), cervical squamous cell carcinoma and endocervical adenocarcinoma (CESC), kidney chromophobe (KICH), and uterine corpus endometrial carcinoma (UCEC) (**Figure 2B**), while no significant difference was detected in bladder urothelial carcinoma (BLCA), esophageal carcinoma (ESCA), glioblastoma multiforme (GBM), lung adenocarcinoma (LUAD), lung squamous cell carcinoma (LUSC), pancreatic adenocarcinoma (PAAD), prostate adenocarcinoma (PRAD), pheochromocytoma and paraganglioma (PCPG), sarcoma (SARC), stomach adenocarcinoma (STAD), thyroid carcinoma (THCA), or thymoma (THYM) (**Figure 2C**). The results of the TCGA analysis were generally consistent with those of previous reports, except for those of ESCA, PAAD, GBM, and STAD, which did not increase. These discrepancies are probably due to the limited number of normal samples in these TCGA datasets, except for the STAD dataset. The prognostic value of TPT1-AS1 in cancers with TPT1-AS1 overexpression (**Figure 2A**) or underexpression (**Figure 2B**) was further assessed. The top 20%

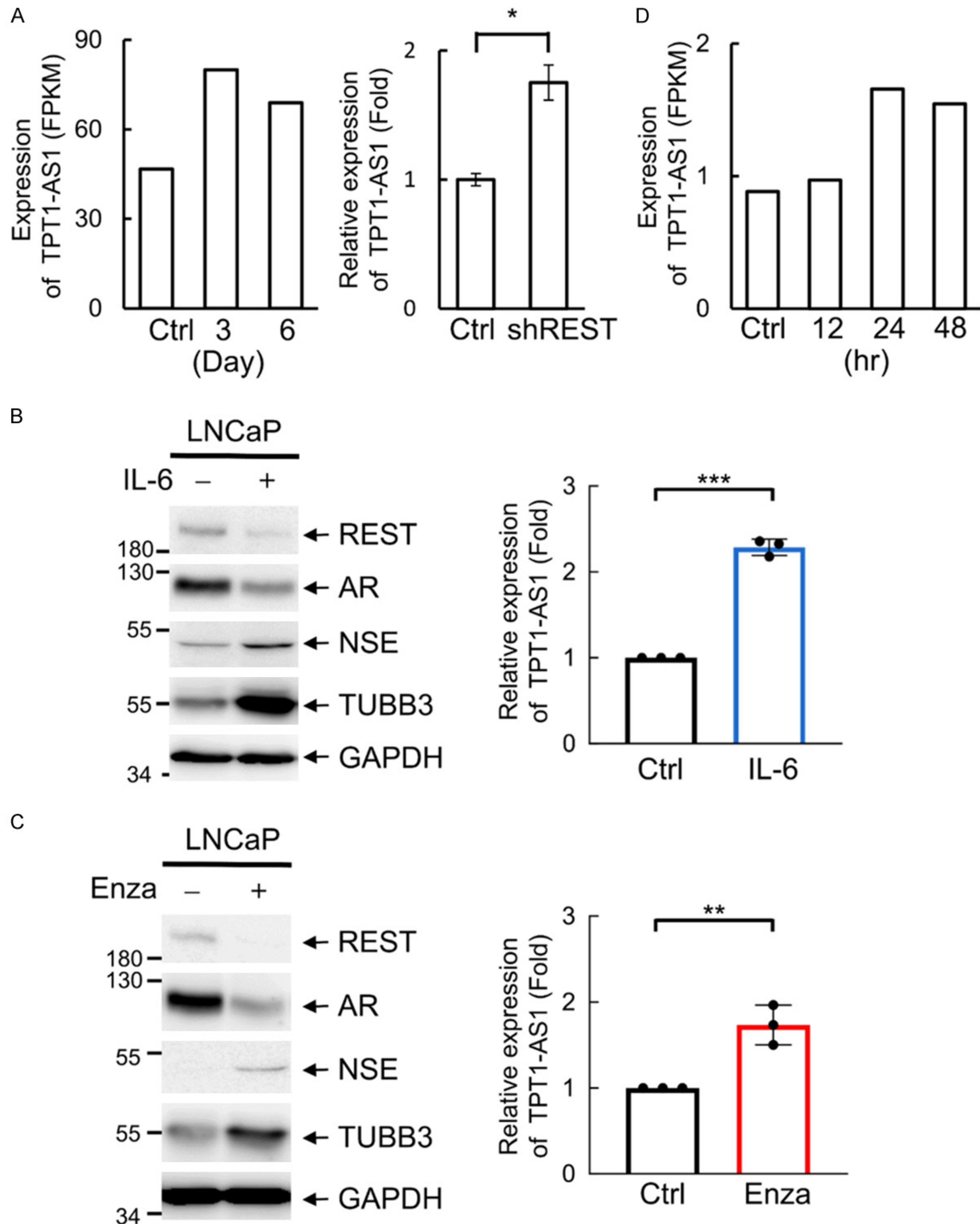

Figure 1. TPT1-AS1 is upregulated in REST knockdown, IL-6-induced and enzalutamide-induced neuroendocrine differentiated LNCaP cells. (A) RNA sequencing (RNA-seq) and RT-qPCR data of LNCaP-TR-shREST cells treated with 1 μg/ml doxycycline (Dox). For RNA-seq, cells were treated for 0, 3, and 6 days (left panel). For RT-qPCR, cells were treated for 0 and 3 days (right panel). (B, C) Immunoblots of REST, AR, and NED markers in LNCaP cells treated with 100 ng/ml IL-6 in phenol red-free RPMI-1640 with 10% CDT (B) and with 50 nM enzalutamide (Enza) (C) for 72 hours (left panel). TPT1-AS1 expression was measured by RT-qPCR (right panel). The cells without treatment were used as the control (Ctrl). GAPDH was used as the loading control. (D) RNA-seq data of LNCaP cells treated with 100 ng/ml IL-6 in phenol red-free RPMI-1640 with 10% CDT for 12, 24, 48 hours. The transcript abundances of RNA-seq data are shown as fragments per kilobase of transcript per million mapped reads (FPKM).

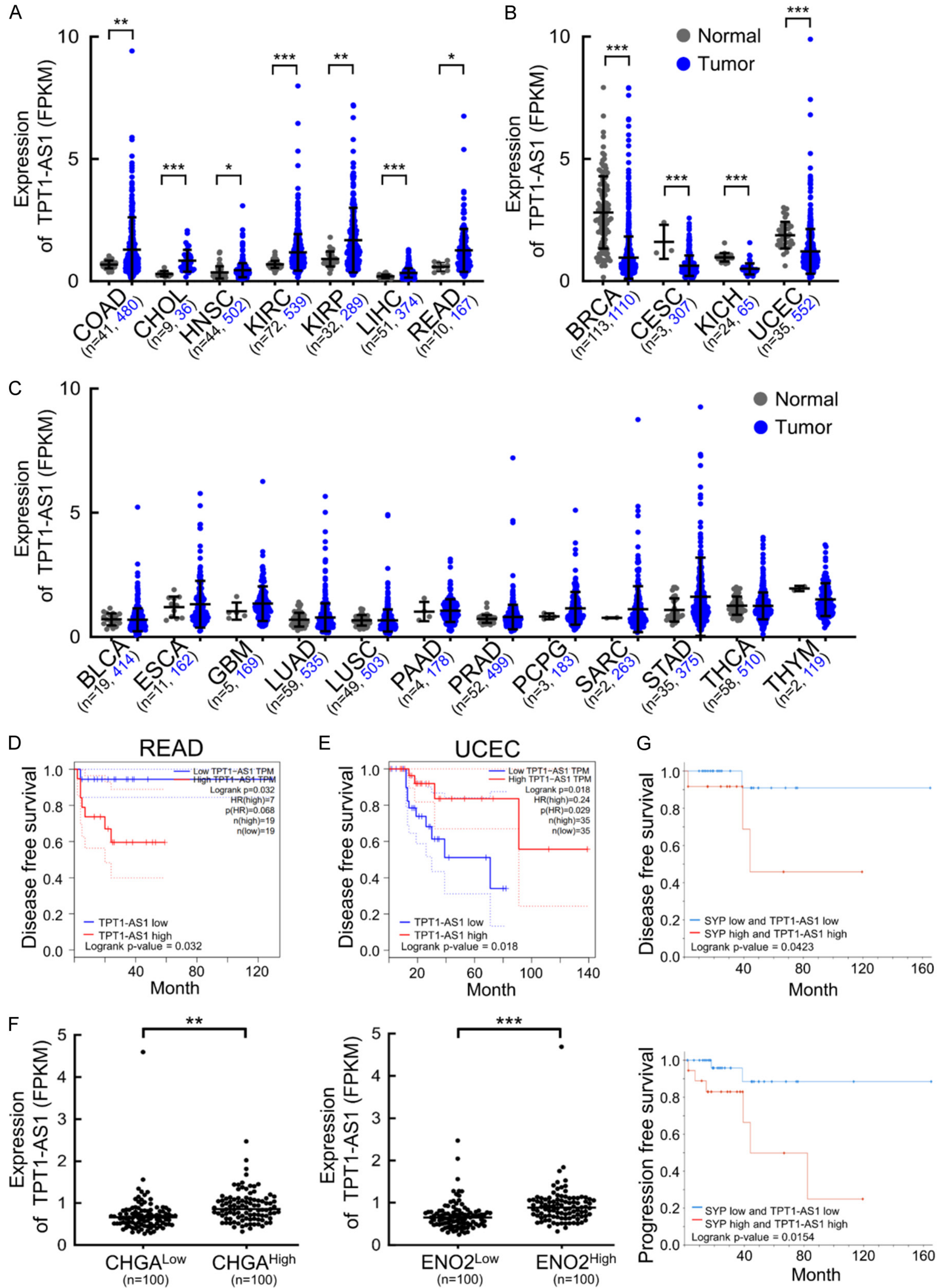

Figure 2. TPT1-AS1 levels are higher in patients with PCA with high levels of neuroendocrine markers. (A-C) Comparison of TPT1-AS1 levels in tumorous and nontumorous tissues from The Cancer Genome Atlas (TCGA) dataset. TPT1-AS1 levels were significantly higher in colon adenocarcinoma (COAD), cholangiocarcinoma (CHOL), head and neck squamous cell carcinoma (HNSC), kidney renal clear cell carcinoma (KIRC), kidney renal papillary cell carci-

noma (KIRP), liver hepatocellular carcinoma (LIHC), and rectum adenocarcinoma (READ) tumorous tissues than in nontumorous tissues (A). TPT1-AS1 levels were significantly lower in breast cancer (BRCA), cervical squamous cell carcinoma and endocervical adenocarcinoma (CESC), kidney chromophobe (KICH), and uterine corpus endometrial carcinoma (UCEC) (B). The TPT1-AS1 levels remained unchanged in bladder urothelial carcinoma (BLCA), esophageal carcinoma (ESCA), glioblastoma multiforme (GBM), lung adenocarcinoma (LUAD), lung squamous cell carcinoma (LUSC), pancreatic adenocarcinoma (PAAD), prostate adenocarcinoma (PRAD), pheochromocytoma and paraganglioma (PCPG), sarcoma (SARC), stomach adenocarcinoma (STAD), thyroid carcinoma (THCA), and thymoma (THYM) (C). (D, E) Kaplan-Meier analysis of TPT1-AS1 in READ (D) and UCEC (E) tissues. The Mantel-Cox test was used to calculate the logarithmic rank *p*-value (*p*-value in each plot). (F) TPT1-AS1 levels were compared between the tumorous samples with high (top 20%) and low (bottom 20%) expression of chromogranin A (CHGA) (left panel) and enolase-2 (ENO2) (right panel) in PRAD dataset from TCGA. (G) TCGA data were analyzed to determine the disease-free survival (top panel) and progression-free survival (bottom panel) of patients in both TPT1-AS1 and synaptophysin (SYP) high/low groups.

of the expression levels were considered high, while the bottom 20% indicated low expression. We found that TPT1-AS1 overexpression predicted poor prognosis in patients with READ (**Figure 2D**), while low TPT1-AS1 expression predicted poor prognosis in patients with UCEC (**Figure 2E**).

Unexpectedly, TPT1-AS1 did not increase in prostate adenocarcinoma (PRAD) tissue compared to normal tissue, suggesting that TPT1-AS1 may not undergo up-regulation in PRAD, but rather increase specifically in NEPC cells. To investigate this possibility, we categorized 499 PRAD samples based on the expression levels of the neuroendocrine markers chromogranin A (CHGA) and enolase-2 (ENO2), also known as neuron-specific enolase (NSE). Using the top 20% of genes with high expression and the bottom 20% with low expression, the analysis demonstrated significant up-regulation of TPT1-AS1 in the high CHGA and ENO2 groups (**Figure 2F**), supporting the association of TPT1-AS1 with neuroendocrine features in PRAD. To assess the prognostic value of TPT1-AS1 in NEPC, we compared patients in whom the expression levels of both TPT1-AS1 and the neuroendocrine marker synaptophysin (SYP) were high (n=20) with patients in whom both were low (n=34) in PRAD. The data indicate that TPT1-AS1 expression was a predictor of disease-free survival and progression-free survival in patients with NEPC (**Figure 2G**).

TPT1-AS1 expression is increased in NEPC

NEPC represents a minor population in PCA. To reveal the increase in TPT1-AS1 expression in NEPC, we downloaded four CRPC samples with an NED phenotype from GEO scRNA sequencing data (GSE137829) [48], performed unsupervised graph-based clustering (**Figure 3A**), and identified luminal cells using pan-epithelial marker EPCAM and its lineage marker KRT8 (**Figure 3B**). Next, we performed another unsupervised graph-based clustering of luminal cells (**Figure 3C**) and identified neuroendocrine clusters using NEURO I and NEURO II markers [12]. Ten luminal clusters were identified, where one demonstrates a high NEURO I score (Cluster 9), two exhibit high NEURO II scores (Clusters 4 and 7), and one displays a high double score (Cluster 5) (**Figure 3D**). As lncRNAs generally exhibit lower expression levels compared to coding RNAs, we examined the expression of TPT1-AS1 in single-cell RNA-seq data by counting cells expressing it. The findings indicated that the group with a high double neuroendocrine score had the highest percentage of cells expressing TPT1-AS1 (**Figure 3E**). To understand the functional characteristics of the population with high TPT1-AS1 expression, we performed Gene Ontology (GO) analysis using biomarkers specific to this cluster by Ingenuity Pathway Analysis (IPA), with a particular emphasis on nervous system signaling, given the neuronal nature of NEPC. Remarkably, our investigation also revealed the enrichment of the autophagy pathway within this cluster, providing valuable insights into the involvement of TPT1-AS1 in modulating the autophagy pathway (**Figure 3F**).

IL-6-induced expression of TPT1-AS1 protects neuroendocrine-differentiated LNCaP cells from cell death

To investigate the role of TPT1-AS1 in NED in PCA, we generated an inducible TPT1-AS1-overexpressing LNCaP cell line. Despite the successful induction of TPT1-AS1 confirmed by RT-qPCR (**Figure 4A**), the immunoblot data surprisingly revealed no increases in the levels of neuroendocrine markers (**Figure 4B**), suggest-

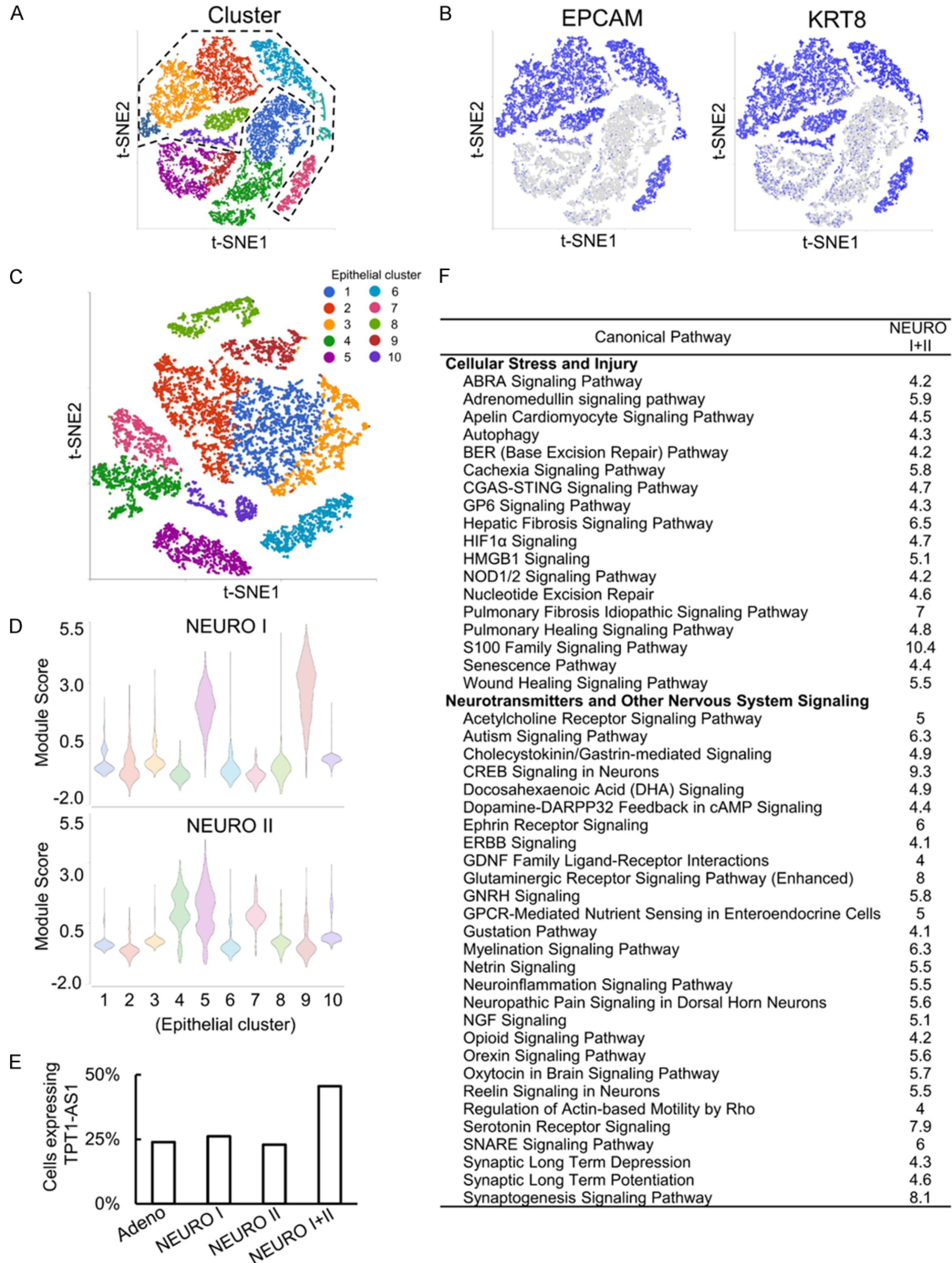

Canonical Pathway	NEURO I+II
Cellular Stress and Injury	
ABRA Signaling Pathway	4.2
Adrenomedullin signaling pathway	5.9
Apelin Cardiomyocyte Signaling Pathway	4.5
Autophagy	4.3
BER (Base Excision Repair) Pathway	4.2
Cachexia Signaling Pathway	5.8
CGAS-STING Signaling Pathway	4.7
GP6 Signaling Pathway	4.3
Hepatic Fibrosis Signaling Pathway	6.5
HIF1α Signaling	4.7
HMGB1 Signaling	5.1
NOD1/2 Signaling Pathway	4.2
Nucleotide Excision Repair	4.6
Pulmonary Fibrosis Idiopathic Signaling Pathway	7
Pulmonary Healing Signaling Pathway	4.8
S100 Family Signaling Pathway	10.4
Senescence Pathway	4.4
Wound Healing Signaling Pathway	5.5
Neurotransmitters and Other Nervous System Signaling	
Acetylcholine Receptor Signaling Pathway	5
Autism Signaling Pathway	6.3
Cholecystokinin/Gastrin-mediated Signaling	4.9
CREB Signaling in Neurons	9.3
Docosahexaenoic Acid (DHA) Signaling	4.9
Dopamine-DARPP32 Feedback in cAMP Signaling	4.4
Ephrin Receptor Signaling	6
ERBB Signaling	4.1
GDNF Family Ligand-Receptor Interactions	4
Glutaminergic Receptor Signaling Pathway (Enhanced)	8
GNRH Signaling	5.8
GPCR-Mediated Nutrient Sensing in Enteroendocrine Cells	5
Gustation Pathway	4.1
Myelination Signaling Pathway	6.3
Netrin Signaling	5.5
Neuroinflammation Signaling Pathway	5.5
Neuropathic Pain Signaling in Dorsal Horn Neurons	5.6
NGF Signaling	5.1
Opioid Signaling Pathway	4.2
Orexin Signaling Pathway	5.6
Oxytocin in Brain Signaling Pathway	5.7
Reelin Signaling in Neurons	5.5
Regulation of Actin-based Motility by Rho	4
Serotonin Receptor Signaling	7.9
SNARE Signaling Pathway	6
Synaptic Long Term Depression	4.3
Synaptic Long Term Potentiation	4.6
Synaptogenesis Signaling Pathway	8.1

Figure 3. TPT1-AS1 expression is increased in the neuroendocrine cell population. A. T-distributed stochastic neighbor embedding (t-SNE) plot of 4 samples from GSE137829, where 17,109 single cells were grouped into 12 clusters and distinguished by different colors. The dashed line box represents the luminal cell population. B. Normalized expression of the pan-epithelial marker EPCAM and the luminal lineage marker keratin 8 (KRT8) overlaid on a tSNE plot. C. Luminal cells were combined and grouped into 10 clusters using graph-based clustering and then visualized in a t-SNE plot with distinct colors representing each luminal cluster. D. Violin plots displaying the scores of NEURO

I panel (neuroendocrine genes repressed by REST) and NEURO II panel (neuroendocrine transcription factors) in luminal cell clusters. E. Percentage of prostate adenocarcinoma (Adeno), NEURO I, NEURO II, and double-positive (NEURO I and NEURO II) populations expressing TPT1-AS1. F. Ingenuity pathway analysis (IPA) was used to reveal functional categories significantly enriched in biomarker genes in the double-positive (NEURO I and NEURO II) population.

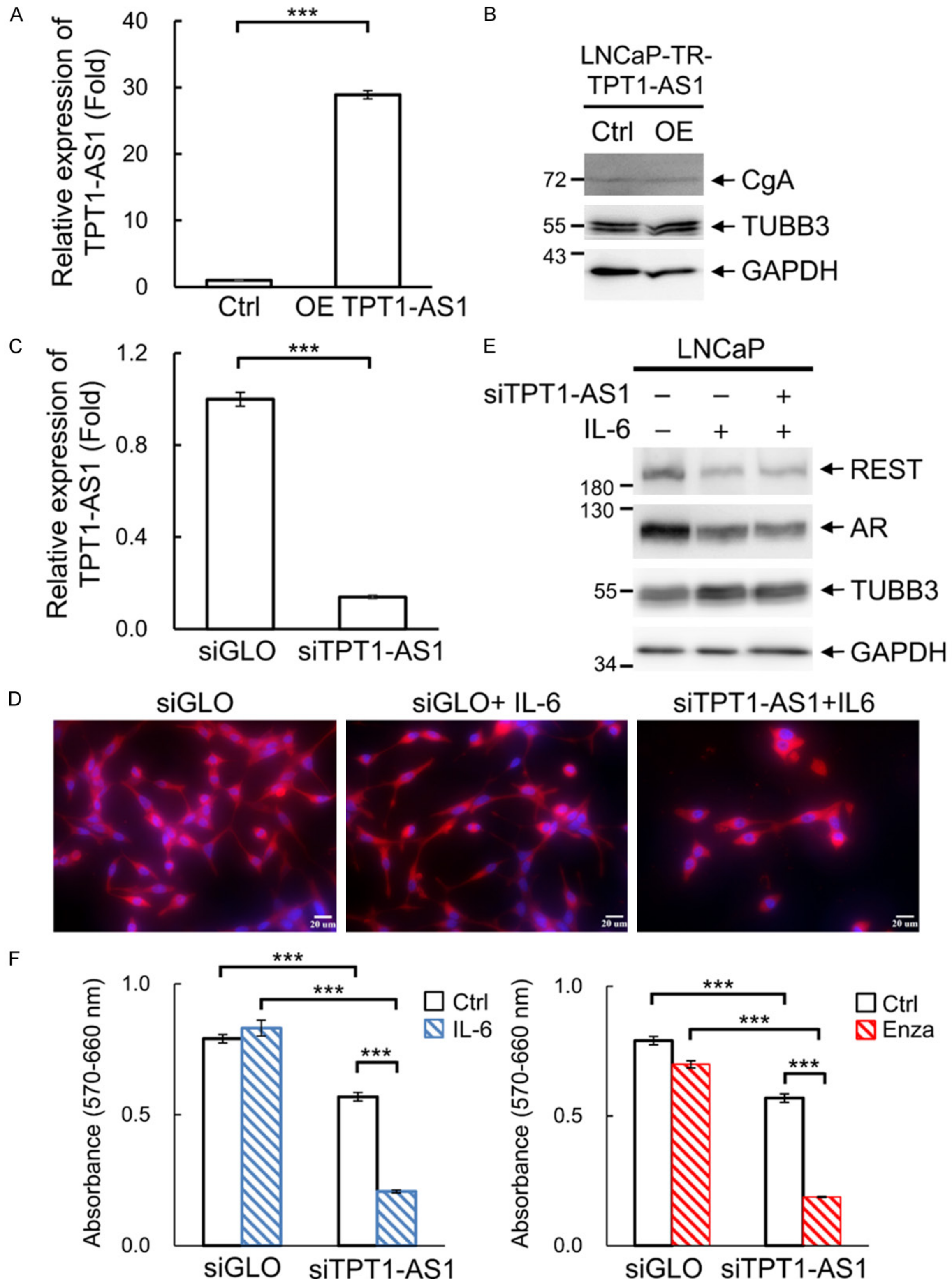

Figure 4. TPT1-AS1 does not affect NED but leads to cell death in neuroendocrine-differentiated LNCaP cells. (A) RT-qPCR analysis was used to assess the expression of TPT1-AS1 in LNCaP-TR-TPT1-AS1 cells treated with 1 μg/ml Dox for 72 hours, with untreated cells serving as the control (Ctrl). (B) Immunoblots of neuroendocrine markers in LNCaP-TR-TPT1-AS1 cells treated as described in (A). GAPDH was used as the loading control. (C) RT-qPCR was performed to detect TPT1-AS1 in LNCaP cells transfected with control siGLO or siRNA targeting TPT1-AS1 (siTPT1-AS1) for 48 hours. (D) LNCaP cells were transfected as described in (C) and then treated with 100 ng/mL IL-6 in phenol red-free RPMI-1640 supplemented with 10% CDT for 72 hours. Representative images (40× magnification) of LNCaP cells stained with a cell membrane stain (red) and with Hoechst33342. (E) Immunoblots of REST, AR, and NED marker tubulin III (TUBIII) in LNCaP cells transfected and treated as described in (D). GAPDH was used as the loading control. (F) LNCaP cells were transfected as described in (C) and then treated with 100 ng/mL IL-6 in phenol red-free RPMI-1640 supplemented with 10% CDT (left panel) or with 50 nM Enza (right panel) for 72 hours. Cells were analyzed using an MTT cell viability assay.

ing that TPT1-AS1 may not directly drive NED. Consequently, we hypothesized that TPT1-AS1 might specifically contribute to IL-6-induced NED. To explore this possibility, we employed an siRNA approach to knock down TPT1-AS1 in LNCaP cells (**Figure 4C**), followed by IL-6 treatment. In line with our screening results [24], TPT1-AS1 knockdown impeded IL-6-induced neuroendocrine-like cell morphology (**Figure 4D**). However, the expression of neuroendocrine markers remained unchanged compared to that in IL-6-treated LNCaP cells (**Figure 4E**). Nevertheless, we observed lower numbers of cells in the TPT1-AS1 knockdown and IL-6 treatment groups (**Figure 4D**), suggesting that while TPT1-AS1 overexpression did not induce NED, it may protect the survival of IL-6-induced neuroendocrine differentiated cells.

To further investigate this possibility, we conducted MTT assays on TPT1-AS1 knockdown LNCaP cells under NED induction conditions, including IL-6 and enzalutamide treatments. Consistent with our hypothesis, TPT1-AS1 knockdown alone led to a slight but significant increase in cell death (**Figure 4F**). Notably, a considerable increase in cell death was observed in cells treated with IL-6 and enzalutamide following TPT1-AS1 knockdown (**Figure 4F**), highlighting the importance of TPT1-AS1 in protecting the survival of NEPC cells.

TPT1-AS1 activates autophagy in IL-6- and enzalutamide-induced NED of PCA

IL-6 concomitantly induces NED and autophagy in PCA cells [16, 29]. However, the role of autophagy in the progression of NED in PCA remains unclear. Moreover, REST-repressed MAOA gene determines the destiny of neuroendocrine cells by orchestrating autophagy and apoptosis - two crucial mechanisms governing cell fate [19]. To elucidate the role of TPT1-AS1 in IL-6-induced NED, we performed RNA sequencing (RNA-seq) of LNCaP cells after TPT1-AS1 knockdown and subsequent IL-6 treatment. RNA-seq analysis revealed 12,065 expressed mRNAs (FPKM>0.5), with 1,988 genes (13%) up-regulated and 1,270 genes (8%) down-regulated after IL-6 treatment. In IL-6-treated TPT1-AS1 knockdown LNCaP cells, 519 genes (4%) were up-regulated, and 1,527 genes (11%) were down-regulated. Then, we performed GO analysis using IPA to identify enriched pathways, with a specific focus on pathways exhibiting opposite regulatory effect between IL-6-treated cells and IL-6-treated TPT1-AS1 knockdown cells. This approach allowed us to elucidate the pathways affected by TPT1-AS1 in response to IL-6 treatment. The positive activation of cytokine signaling, including IL-6 signaling; nervous system signaling, such as synaptogenesis signaling; and cancer-related pathways provides insights into the involvement of TPT1-AS1 in IL-6-induced NED in PCA (**Table 1**). Notably, the autophagy pathway, which is known to be activated by IL-6, was also down-regulated after TPT1-AS1 was knocked down, highlighting the potential interplay between TPT1-AS1 and autophagy in the context of IL-6-induced NED.

To validate whether TPT1-AS1 also induces autophagy in the context of enzalutamide-induced NED of PCA, we performed additional RNA-seq analysis in LNCaP cells following TPT1-AS1 knockdown and subsequent enzalutamide treatment. RNA-seq revealed 12,166 expressed mRNAs (FPKM>0.5), with 2,229 upregulated genes (18%) and 1,177 down-regulated genes (9%) after enzalutamide treatment. In enzalutamide-treated TPT1-AS1 knockdown LNCaP cells, 511 genes (4%) were up-regulated and 1,763 genes (14%) were down-regulated. Subsequently, we performed

Table 1. GO categories of TPT1-AS1-regulated genes upon IL-6 and enzalutamide treatment

Canonical Pathway	LNCaP IL-6		LNCaP Enza	
	siCtrl	SITPT1-AS1	siCtrl	SITPT1-AS1
Cytokine Signaling				
Dendritic Cell Maturation	4.23	-3.3	-	-
IL-15 Production	3.53	-3	3.41	-3.61
IL-6 Signaling	3.53	-2.14	3.55	-2.89
Interleukin-1 family signaling	2.99	-2.53	3.74	-2.65
Interleukin-15 signaling	2	-2	-	-
Role of JAK family kinases in IL-6-type Cytokine Signaling	2.68	-2.33	-	-
TREM1 Signaling	2.53	-2.24	2.24	-
Cellular Stress and Injury				
Adrenomedullin signaling pathway	3.67	-2.99	-	-
Autophagy	3.86	-2.29	3	-
Cachexia Signaling Pathway	3.79	-2.12	-	-
Ferroptosis Signaling Pathway	2.54	-3.15	2.75	-
Immunogenic Cell Death Signaling Pathway	2.84	-2.24	-	-2.24
NOD1/2 Signaling Pathway	2.12	-2.67	-	-
Pulmonary Fibrosis Idiopathic Signaling Pathway	3.25	-2.19	3.58	-2.67
S100 Family Signaling Pathway	3.44	-3.1	-	-
Neurotransmitters and Other Nervous System Signaling				
Cholecystokinin/Gastrin-mediated Signaling	4.04	-2.18	3.27	-2.5
CREB Signaling in Neurons	3.4	-3.46	5.37	-5.76
Dopamine-DARPP32 Feedback in cAMP Signaling	2.36	-2.71	-	-2.18
Endocannabinoid Neuronal Synapse Pathway	2.36	-2.11	2.24	-
GNRH Signaling	3.66	-3.44	3.8	-2.67
GPCR-Mediated Nutrient Sensing in Enteroendocrine Cells	2.84	-2.71	3.84	-3.15
Gustation Pathway	2.12	-3.27	2.71	-2.24
Netrin Signaling	2.5	-3.15	2.65	-2.68
NGF Signaling	3.4	-2.32	3.3	-2.89
Orexin Signaling Pathway	3.28	-2.89	4.42	-3.77
SNARE Signaling Pathway	2.52	-2.53	3.5	-2.31
Synaptogenesis Signaling Pathway	2.94	-2.61	3.81	-3.54
Cancer				
Cachexia Signaling Pathway	3.79	-2.12	-	-3.77
Colorectal Cancer Metastasis Signaling	4.73	-2.13	3.21	-2.86
FAK Signaling	4.88	-3.97	6.21	-5.66
Molecular Mechanisms of Cancer	5.4	-4.05	5.92	-5.46
PTEN Signaling	-2.5	2.14	-	-
S100 Family Signaling Pathway	3.44	-3.1	5.51	-5.46

GO analysis, focusing on pathways associated with IL-6 treatment, including pathways involved in cytokine signaling, nervous system signaling, cancer, and autophagy. Although not all IL-6 treatment-enriched pathways were activated by enzalutamide, similar results were observed. Most importantly, knockdown of TPT1-AS1 via siRNA abolished the increase in autophagy pathway enriched by enzalutamide treatment (**Table 1**). These findings collectively suggest that TPT1-AS1 plays a role in activating autophagy during NED.

TPT1-AS1 is required for autophagy activation by IL-6 and enzalutamide

To elucidate whether TPT1-AS1 is indeed required for IL-6- and enzalutamide-induced

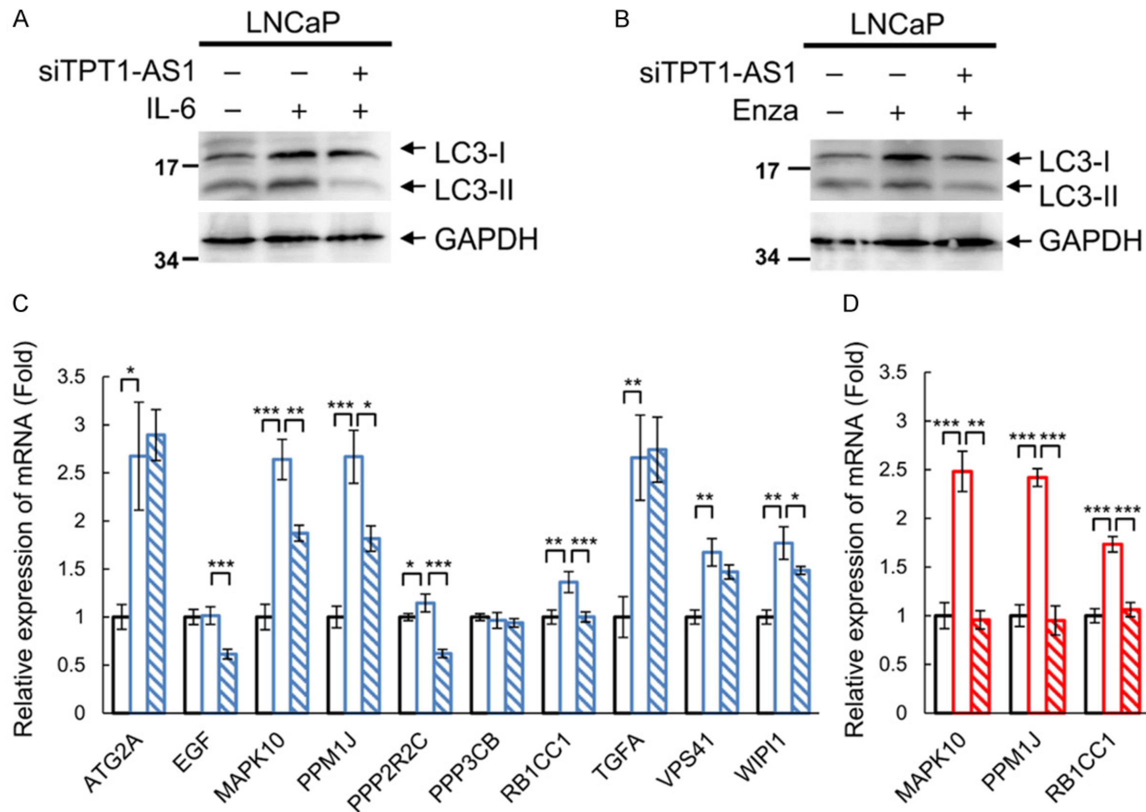

Figure 5. TPT1-AS1 is required for autophagy activation induced by IL-6 and enzalutamide in LNCaP cells. (A) Immunoblots of LC3 in LNCaP cells transfected with siTPT1-AS1 or siGLO for 48 hours and then treated with 100 ng/mL IL-6 in phenol red-free RPMI-1640 supplemented with 10% CDT for 72 hours. GAPDH was used as the loading control. (B) Immunoblots of LC3 in LNCaP cells transfected as described in (A) and then treated with 50 nM Enza for 72 hours. GAPDH was used as the loading control. (C) RT-qPCR was used to detect the expression levels of 10 autophagy-related genes in LNCaP cells treated as described in (A). (D) RT-qPCR was used to detect the expression levels of 3 autophagy-related genes in LNCaP cells treated as described in (B).

autophagy activation, we used siRNA to knock down TPT1-AS1 in LNCaP cells. TPT1-AS1 knockdown attenuated IL-6-induced autophagy, as evidenced by decreased levels of LC3-II (**Figure 5A**), in LNCaP cells. Similarly, TPT1-AS1 knockdown reduced the autophagy induced by enzalutamide treatment (**Figure 5B**). These findings are consistent with previous reports showing that autophagy is activated in neuroendocrine cells induced by IL-6 [16, 29] and enzalutamide [49].

Given that IPA analysis revealed an association between TPT1-AS1 and autophagy, the expression levels of 12 genes involved in the autophagy pathway were assessed using RT-qPCR. The results demonstrated that IL-6 treatment increased the expression of ATG2A, MAPK10, PPM1J, RB1CC1, TGFA, VPS41, and WIPI1 (**Figure 5C**). Subsequently, TPT1-AS1 knockdown significantly attenuated IL-6-induced expression of MAPK10, PPM1J, and RB1CC1 (**Figure 5C**). To further investigate whether MAPK10, PPM1J, and RB1CC1 are also activated by enzalutamide and whether TPT1-AS1 is essential for their activation under enzalutamide treatment conditions, similar experiments were performed. The results showed that enzalutamide treatment activated MAPK10, PPM1J, and RB1CC1, and TPT1-AS1 knockdown abolished this activation (**Figure 5D**). Notably, the impact of TPT1-AS1 on the activation of these autophagy-related genes was more pronounced in the context of enzalutamide treatment. Collectively, these findings further support the notion that TPT1-AS1 is involved in autophagy activation by up-regulating the expression of autophagy-related genes.

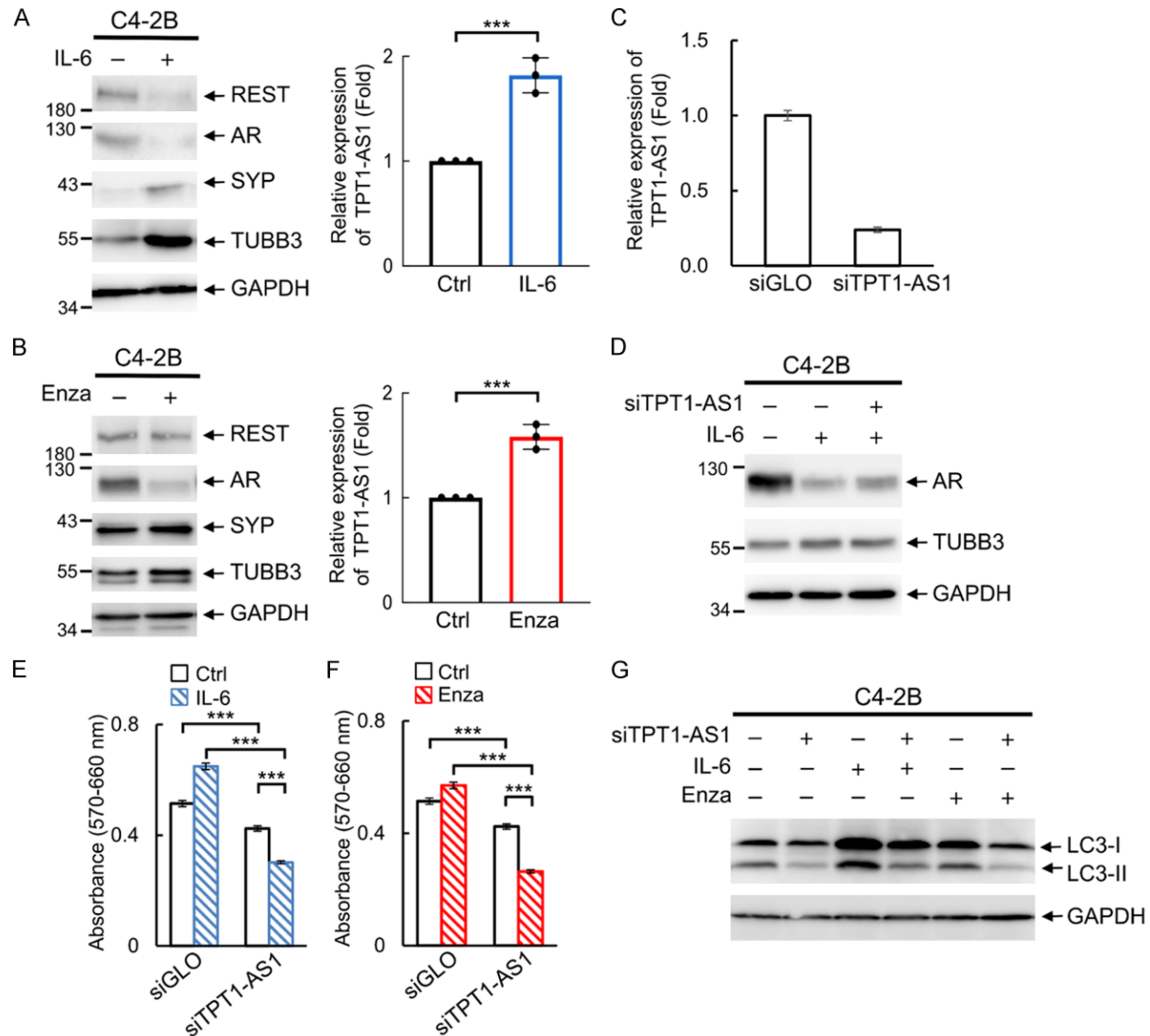

Figure 6. TPT1-AS1 upregulation is essential for autophagy activation and cell survival under IL-6 and Enza treatment in C4-2B cells. (A, B) Immunoblots of REST, AR, and NED markers in C4-2B cells treated with 100 ng/ml IL-6 in phenol red-free RPMI-1640 supplemented with 10% CDT (A) and with 50 nM Enza (B) for 72 hours (left panel). The expression level of TPT1-AS1 was measured by RT-qPCR (right panel). Untreated cells were used as the control (Ctrl). GAPDH was used as the loading control. (C) C4-2B cells were transfected with siTPT1-AS1 or siGLO for 48 hours. RT-qPCR was performed to detect TPT1-AS1 in C4-2B cells. (D) Immunoblots of AR and TUBIII in C4-2B cells transfected with siTPT1-AS1 or siGLO for 48 hours and then treated with 100 ng/mL IL-6 in phenol red-free RPMI-1640 supplemented with 10% CDT for 72 hours. GAPDH was used as the loading control. (E) C4-2B cells, transfected and treated as described in (D), were analyzed by MTT cell viability assay. *Bars*, SD. (F) C4-2B cells were transfected as described in (D) and then treated with 50 nM enzalutamide (Enza) for 72 hours. Cell numbers were analyzed using an MTT cell viability assay. *Bars*, SD. (G) Immunoblots of LC3 in C4-2B cells transfected with siTPT1-AS1 or siGLO for 48 hours and then treated with 100 ng/mL IL-6 in phenol red-free RPMI-1640 supplemented with 10% CDT or 50 nM Enza for 72 hours. GAPDH was used as the loading control.

Validation of TPT1-AS1 upregulation and its cytoprotective role in neuroendocrine differentiated C4-2B cells

In this section, we aimed to confirm the involvement/role of TPT1-AS1 in NED using C4-2B cells, a CRPC subline derived from LNCaP cells. First, we assessed whether TPT1-AS1 is upregulated under NED induction conditions, focusing on IL-6 and enzalutamide treatments (**Figure 6A** and **6B**, left panel). Consistent with our findings in LNCaP cells (**Figure 1**), RT-qPCR analysis confirmed that TPT1-AS1 expression increased following both IL-6 and enzalutamide treatments in C4-2B cells (**Figure 6A** and **6B**, right panel). Second, we used siRNA to knock-

down TPT1-AS1 expression in C4-2B cells (**Figure 6C**) and treated the cells with IL-6. Although IL-6 induced only a slight increase in the expression of neuroendocrine markers in C4-2B cells, TPT1-AS1 knockdown consistently exhibited no alteration in this neuroendocrine induction (**Figure 6D**). Third, we conducted MTT assays on TPT1-AS1 knockdown C4-2B cells under NED induction conditions, including IL-6 and enzalutamide treatments. In agreement with our observations in LNCaP cells (**Figure 4F**), TPT1-AS1 knockdown resulted in a slight increase in cell death (**Figure 6E** and **6F**), while a considerable increase in cell death was noted in cells treated with IL-6 and enzalutamide following TPT1-AS1 knockdown (**Figure 6E** and **6F**), highlighting the importance of TPT1-AS1 in protecting the survival of NEPC cells differentiated from CRPC cells. Finally, we validated whether TPT1-AS1 is indispensable for the activation of IL-6- and enzalutamide-induced autophagy in C4-2B cells. To test this possibility, we knocked down TPT1-AS1 in C4-2B cells, followed by treatment with IL-6 and enzalutamide. Consistently, TPT1-AS1 attenuated autophagy induced by IL-6 and enzalutamide treatment (**Figure 6G**).

Discussion

NEPC, which was once an infrequent phenomenon, has become increasingly prevalent due to the widespread use of new-generation ARIs. Furthermore, pathogenic conditions, such as hypoxia [18] and elevated serum levels of IL-6 in patients with CRPC and metastatic PCA after androgen-deprivation therapy [50-52], have also been identified as inducers of NED in PCA cells [16, 18, 29]. Given the lethality of NEPC and the current lack of effective treatment options, extensive research has been devoted to understanding the molecular mechanisms underlying its evolution. In addition to genetic mutations and amplifications [53, 54], epigenetic regulation of chromatin accessibility for transcription has become another pivotal factor in NEPC [55]. More importantly, unlike irreversible genetic events with limited targeted therapy options, the role of epigenetics in driving disease progression holds particular interest, as its potential reversibility and susceptibility to target by epigenetic enzymes.

REST serves as a master epigenetic repressor that governs the expression of NED driver genes in PCA [16-18]. Down-regulation of REST, a transcriptional repressor known to regulate neuronal differentiation [56] and tumor growth [57], has been observed in up to 50% of clinical NEPC specimens [58]. However, the mechanisms underlying the role of REST in regulating NED in PCA remain to be elucidated. To address this issue, we performed a bioinformatic analysis of transcriptomic data and revealed that, in addition to targeting neuronal-related genes, REST also regulates autophagy-related genes [16] and the mitochondrial outer membrane-bound enzyme MAOA. MAOA participates in inhibiting apoptosis and activating autophagy [19]. These data suggest that autophagy is activated simultaneously with NED in PCA.

Importantly, the epigenetic/non-coding interactome is emerging as a novel mechanism orchestrating the initiation and progression of NEPC [59]. Given the relatively high tissue specificity of lncRNAs, exploring NEPC-associated lncRNAs holds promise for identifying specific diagnostic, prognostic, and therapeutic targets for NEPC. One promising example is the FDA-approved lncRNA biomarker, prostate cancer gene 3 (PCA3), which is now routinely used to diagnose PCA [60, 61]. Therefore, we hypothesized that REST might also play a pivotal role in the negative regulation of lncRNAs with NED-driving potential. The down-regulation of REST during NED may concomitantly up-regulate the expression of those lncRNAs and consequently induce NED. To identify lncRNAs as potential drivers of NED, we reannotated our transcriptome data using the non-coding RNA database, NONCODEv4 [62], and identified lncRNAs that are up-regulated after REST knockdown and concurrent NED. Using the siRNA knockdown approach, we validated HOTAIR [23] and LINC01801 [24] as novel neuroendocrine-associated lncRNAs. Notably, overexpression of both HOTAIR and LINC01801 not only induces NED in PCA cells but also regulates genes enriched in the autophagy pathway [23, 24]. Collectively, our study highlighted that REST may concomitantly induce NED and autophagy by derepressing both coding and noncoding RNAs.

Our previous study involving REST knockdown transcriptomic analysis combined with siRNA screening also identified TPT1-AS1 as another potential REST-repressed neuroendocrine-associated lncRNA [24]. TPT1-AS1 has been

studied extensively and is recognized as a tumor-associated lncRNA with varying expression levels in different types of cancer [38-47, 63]. To comprehensively assess its expression in various cancers, we analyzed TPT1-AS1 levels in clinical samples from the TCGA database. Among the 33 cancers analyzed, only 23 had corresponding normal tissue data. The analysis revealed that TPT1-AS1 is overexpressed in cholangiocarcinoma and colorectal, liver, and head and neck cancers (**Figure 2A**), while it is down-regulated in breast, cervical, and endometrial cancers (**Figure 2B**). Interestingly, among the three types of kidney cancer, TPT1-AS1 exhibited variable expression and was overexpressed in KIRC and KIRP but down-regulated in KICH (**Figure 2A** and **2B**). Furthermore, our TCGA data indicated that TPT1-AS1 levels in PCA were similar between normal and cancerous tissues (**Figure 2C**). However, when we subgrouped them by neuroendocrine markers, we observed an overexpression of TPT1-AS1 in NEPC (**Figure 2D**). These findings support the necessity of separately elucidating the tumorigenic role of TPT1-AS1 in different types and subtypes of cancer. More interestingly, lncRNAs, particularly TPT1-AS1, have been recognized to regulate transcription by acting as competitive endogenous RNAs (ceRNAs) that sponge miRNAs [34]. Notably, in breast cancer, TPT1-AS1 has been identified as a sponge for miR-3156-5p and miR-330-3p, resulting in up-regulation of CASP2 and QKI, respectively [44, 45]. In glioma, TPT1-AS1 promotes cell proliferation by sponging miR-23a-5p and miR-770-5p, leading to the up-regulation of ECM1 and STMN1, respectively [43, 64]. In pancreatic cancer, TPT1-AS1 acts as a sponge for miR-30a-5p, contributing to the up-regulation of ITGB3 [40]. Similarly, in esophageal cancer, TPT1-AS1 functions as a sponge for miR-26a, resulting in the up-regulation of HMGA1 [42]. These findings suggest that TPT1-AS1 modulates gene expression by interacting with multiple miRNAs.

Given that lncRNAs modulate gene transcription by sponging miRNAs, their expression can lead to coup- and codown-regulation of target genes. This phenomenon may hold true in PCA cells treated with IL-6 and enzalutamide, as the sequence results showed that under IL-6 treatment conditions, more genes were up-regulated (1,988; 13%) than down-regulated (1,270; 8%). Notably, TPT1-AS1 knockdown under IL-6 treatment conditions significantly increased the number of down-regulated genes (1,527; 11%) compared to up-regulated genes (519; 4%). Similarly, in enzalutamide treatment group, more genes were up-regulated (2,229; 18%) than down-regulated (1,177; 9%). Once again, TPT1-AS1 knockdown under enzalutamide treatment conditions led to a notable increase in down-regulated genes (1,763; 14%) compared to up-regulated genes (511; 4%). These observations imply a potential interplay between TPT1-AS1 and miRNAs in the context of IL-6 and enzalutamide treatments in PCA cells.

Moreover, in our study, IL-6 and enzalutamide treatment increased the expression levels of autophagy-related genes MAPK10, PPM1J, and RB1CC1, while TPT1-AS1 knockdown attenuated their expression (**Figure 5C** and **5D**). To explore whether MAPK10, PPM1J, and RB1CC1 are potential targets of TPT1-AS1-associated miRNAs, we performed miRNA prediction using TarBase-v9.0 [65]. The prediction results showed that hsa-miR-30a-5p and hsa-miR-26a-5p could target all three identified autophagy-related genes. Additionally, RB1CC1 was also predicted to be targeted by hsa-miR-330-3p. Collectively, these data indicate a potential regulatory axis involving TPT1-AS1, miRNAs, and autophagy-related genes in the context of IL-6 and enzalutamide treatments in PCA cells. Further exploration of these interactions may provide valuable insights into the molecular mechanisms underlying PCA progression.

In this study, our focus was to elucidate the role of TPT1-AS1, a REST-repressed lncRNA, in the NED of PCA. Surprisingly, while the overexpression of TPT1-AS1 was evident in NEPC cells (**Figure 1**) and neuroendocrine-associated PCA (**Figure 2D**), no NED induction was observed after overexpression of TPT1-AS1 (**Figure 4A** and **4B**). Moreover, TPT1-AS1 knockdown did not abolish IL-6-induced NED in LNCaP cells (**Figure 4C-E**). However, a notable increase in cell death was observed in LNCaP cells after TPT1-AS1 knockdown, particularly in IL-6-treated cells. This led us to hypothesize that TPT1-AS1 may not directly contribute to NED in PCA cells; instead, its upregulation might activate a cell protective mechanism preventing neuroendocrine cell death under

neuroendocrine induction conditions. Indeed, survival assays demonstrated that TPT1-AS1 knockdown alone caused slight cell death, while a significant increase in cell death was observed in TPT1-AS1 knockdown cells treated with IL-6 or enzalutamide (**Figure 4F**). Taken together, our findings suggest that using an siRNA-mediated knockdown approach to identify neuroendocrine-associated lncRNAs can reveal lncRNAs involved in maintaining cell survival rather than promoting NED in PCA cells. The knockdown of these lncRNAs resulted in neuroendocrine cell death and the absence of NED characteristics. This observation aligns with studies that have questioned the role of HOTAIR as a driver of NED in PCA [66]. Most importantly, the induction of TPT1-AS1 in triple-negative breast cancer in response to DNA methyltransferase (DNMT) inhibition [63] suggests promising therapeutic opportunities by targeting DNA demethylation to modulate TPT1-AS1 expression.

To explore the potential mechanisms underlying the protective role of TPT1-AS1, we conducted transcriptome analysis of IL-6- and enzalutamide-treated LNCaP cells, with or without TPT1-AS1 knockdown. Consistent with previous findings, our treatment induced changes in neuronal-related pathways and the autophagy pathway (**Table 1**). Notably, TPT1-AS1 knockdown abolished or even inhibited IL-6- and enzalutamide-induced synaptogenesis and autophagy (**Table 1**). This finding was confirmed using LC3-II as an autophagy activation marker, demonstrating that TPT1-AS1 knockdown eliminated autophagy activation induced by IL-6 (**Figure 5A**) and enzalutamide (**Figure 5B**), potentially through the up-regulation of multiple autophagy-related genes (**Figure 5C**, **5D**). As TPT1-AS1 is a well-established ceRNA that sponges numerous miRNAs and many of these miRNAs target autophagy-related genes regulated by TPT1-AS1 under neuroendocrine induction conditions, our data suggest that TPT1-AS1 may modulate autophagy by acting as an miRNA sponge. Further exploration is warranted to elucidate these intricate interactions.

In conclusion, we identified TPT1-AS1 as a novel REST-repressed lncRNA that is overexpressed in neuroendocrine-associated PCA. TPT1-AS1 plays crucial roles in inducing autophagy-related genes, activating autophagy, and promoting cell survival in IL-6- and enzalutamide-induced NEPC cells. These findings suggest that TPT1-AS1 is a potential prognostic biomarker for NEPC and highlight TPT1-AS1 as a promising therapeutic target for NEPC.

Acknowledgements

The authors acknowledge the technical services provided by the National Genomics Center for Clinical and Biotechnological Applications of the Cancer Progression Research Center (National Yang Ming Chiao Tung University), the National Core Facility for Biopharmaceuticals (NCFB), and the National Science and Technology Council (NSTC 112-2740-B-A49-001, NSTC 111-2740-B-A49-001). This work was supported by grants to T.P.L. (MOST 109-2314-B-075-072-MY3; NSTC 112-2314-B-A49-055-MY3; NHRI NHRI-109BCCO-MF-202014-03; and Taipei Veterans General Hospital, V112C-077, V113C-075) and grants to P.C.C. (NSTC 111-2320-B-A49-030-MY3 and 112-2314-B-A49-023-MY3; and NHRI NHRI-EX111~113-11125BI), and grants from the Prof. Albert Ly-Young Shen's Medical Education Foundation, Melissa Lee Cancer Foundation, R & D Foundation of Urological Medicine, Ministry of Education, Higher Education SPROUT Project for Cancer Progression Research Center (111W31101) and the Cancer and Immunology Research Center (112W31101 and 113W031101).

Disclosure of conflict of interest

None.

Address correspondence to: Tzu-Ping Lin, Department of Urology, Taipei Veterans General Hospital, Taipei 11217, Taiwan. Tel: +886-2-2875-7519; E-mail: tplin@vghtpe.gov.tw

References

[1] Abida W, Cyrta J, Heller G, Prandi D, Armenia J, Coleman I, Cieslik M, Benelli M, Robinson D, Van Allen EM, Sboner A, Fedrizzi T, Mosquera JM, Robinson BD, De Sarkar N, Kunju LP, Tomlins S, Wu YM, Nava Rodrigues D, Loda M, Gopalan A, Reuter VE, Pritchard CC, Mateo J, Bianchini D, Miranda S, Carreira S, Rescigno P, Filipenko J, Vinson J, Montgomery RB, Beltran H, Heath EI, Scher HI, Kantoff PW, Taplin ME, Schultz N, deBono JS, Demichelis F, Nelson PS, Rubin MA, Chinnaiyan AM and Sawyers CL. Genomic correlates of clinical outcome in advanced prostate cancer. Proc Natl Acad Sci U S A 2019; 116: 11428-11436.

[2] Aggarwal R, Huang J, Alumkal JJ, Zhang L, Feng FY, Thomas GV, Weinstein AS, Friedl V, Zhang C, Witte ON, Lloyd P, Gleave M, Evans CP, Youngren J, Beer TM, Rettig M, Wong CK, True L, Foye A, Playdle D, Ryan CJ, Lara P, Chi KN, Uzunangelov V, Sokolov A, Newton Y, Beltran H, Demichelis F, Rubin MA, Stuart JM and Small EJ. Clinical and genomic characterization of treatment-emergent small-cell neuroendocrine prostate cancer: a multi-institutional prospective study. J Clin Oncol 2018; 36: 2492-2503.

[3] Rickman DS, Beltran H, Demichelis F and Rubin MA. Biology and evolution of poorly differentiated neuroendocrine tumors. Nat Med 2017; 23: 1-10.

[4] Davies AH, Beltran H and Zoubeidi A. Cellular plasticity and the neuroendocrine phenotype in prostate cancer. Nat Rev Urol 2018; 15: 271-286.

[5] Cui Y, Sun Y, Hu S, Luo J, Li L, Li X, Yeh S, Jin J and Chang C. Neuroendocrine prostate cancer (NEPCa) increased the neighboring PCa chemoresistance via altering the PTHrP/p38/Hsp27/androgen receptor (AR)/p21 signals. Oncogene 2016; 35: 6065-6076.

[6] Puca L, Vlachostergios PJ and Beltran H. Neuroendocrine differentiation in prostate cancer: emerging biology, models, and therapies. Cold Spring Harb Perspect Med 2019; 9: a030593.

[7] de Bono JS, Logothetis CJ, Molina A, Fizazi K, North S, Chu L, Chi KN, Jones RJ, Goodman OB Jr, Saad F, Staffurth JN, Mainwaring P, Harland S, Flaig TW, Hutson TE, Cheng T, Patterson H, Hainsworth JD, Ryan CJ, Sternberg CN, Ellard SL, Flechon A, Saleh M, Scholz M, Efstathiou E, Zivi A, Bianchini D, Loriot Y, Chieffo N, Kheoh T, Haqq CM and Scher HI; COU-AA-301 Investigators. Abiraterone and increased survival in metastatic prostate cancer. N Engl J Med 2011; 364: 1995-2005.

[8] Scher HI, Fizazi K, Saad F, Taplin ME, Sternberg CN, Miller K, de Wit R, Mulders P, Chi KN, Shore ND, Armstrong AJ, Flaig TW, Flechon A, Mainwaring P, Fleming M, Hainsworth JD, Hirmand M, Selby B, Seely L and de Bono JS; AFFIRM Investigators. Increased survival with enzalutamide in prostate cancer after chemotherapy. N Engl J Med 2012; 367: 1187-1197.

[9] Hashimoto K, Kyoda Y, Tanaka T, Maeda T, Kobayashi K, Uchida K, Kitamura H, Hirata K, Tsukamoto T and Masumori N. The potential of neurotensin secreted from neuroendocrine tumor cells to promote gelsolin-mediated invasiveness of prostate adenocarcinoma cells. Lab Invest 2015; 95: 283-295.

[10] Beltran H, Hruszkewycz A, Scher HI, Hildesheim J, Isaacs J, Yu EY, Kelly K, Lin D, Dicker A, Arnold J, Hecht T, Wicha M, Sears R, Rowley D, White R, Gulley JL, Lee J, Diaz Meco M, Small EJ, Shen M, Knudsen K, Goodrich DW, Lotan T, Zoubeidi A, Sawyers CL, Rudin CM, Loda M, Thompson T, Rubin MA, Tawab-Amiri A, Dahut W and Nelson PS. The role of lineage plasticity in prostate cancer therapy resistance. Clin Cancer Res 2019; 25: 6916-6924.

[11] Beltran H, Prandi D, Mosquera JM, Benelli M, Puca L, Cyrta J, Marotz C, Giannopoulou E, Chakravarthi BV, Varambally S, Tomlins SA, Nanus DM, Tagawa ST, Van Allen EM, Elemento O, Sboner A, Garraway LA, Rubin MA and Demichelis F. Divergent clonal evolution of castration-resistant neuroendocrine prostate cancer. Nat Med 2016; 22: 298-305.

[12] Labrecque MP, Coleman IM, Brown LG, True LD, Kollath L, Lakely B, Nguyen HM, Yang YC, da Costa RMG, Kaipainen A, Coleman R, Higano CS, Yu EY, Cheng HH, Mostaghel EA, Montgomery B, Schweizer MT, Hsieh AC, Lin DW, Corey E, Nelson PS and Morrissey C. Molecular profiling stratifies diverse phenotypes of treatment-refractory metastatic castration-resistant prostate cancer. J Clin Invest 2019; 129: 4492-4505.

[13] Berger A, Brady NJ, Bareja R, Robinson B, Conteduca V, Augello MA, Puca L, Ahmed A, Dardenne E, Lu X, Hwang I, Bagadion AM, Sboner A, Elemento O, Paik J, Yu J, Barbieri CE, Dephoure N, Beltran H and Rickman DS. N-Myc-mediated epigenetic reprogramming drives lineage plasticity in advanced prostate cancer. J Clin Invest 2019; 129: 3924-3940.

[14] Lee JK, Phillips JW, Smith BA, Park JW, Stoyanova T, McCaffrey EF, Baertsch R, Sokolov A, Meyerowitz JG, Mathis C, Cheng D, Stuart JM, Shokat KM, Gustafson WC, Huang J and Witte ON. N-Myc drives neuroendocrine prostate cancer initiated from human prostate epithelial cells. Cancer Cell 2016; 29: 536-547.

[15] Mosquera JM, Beltran H, Park K, MacDonald TY, Robinson BD, Tagawa ST, Perner S, Bismar TA, Erbersdobler A, Dhir R, Nelson JB, Nanus DM and Rubin MA. Concurrent AURKA and MYCN gene amplifications are harbingers of lethal treatment-related neuroendocrine prostate cancer. Neoplasia 2013; 15: 1-10.

[16] Chang PC, Wang TY, Chang YT, Chu CY, Lee CL, Hsu HW, Zhou TA, Wu Z, Kim RH, Desai SJ, Liu S and Kung HJ. Autophagy pathway is required for IL-6 induced neuroendocrine differentiation and chemoresistance of prostate cancer LNCaP cells. PLoS One 2014; 9: e88556.

[17] Svensson C, Ceder J, Iglesias-Gato D, Chuan YC, Pang ST, Bjartell A, Martinez RM, Bott L, Helczynski L, Ulmert D, Wang Y, Niu Y, Collins C and Flores-Morales A. REST mediates androgen receptor actions on gene repression and

predicts early recurrence of prostate cancer. Nucleic Acids Res 2014; 42: 999-1015.
[18] Lin TP, Chang YT, Lee SY, Campbell M, Wang TC, Shen SH, Chung HJ, Chang YH, Chiu AW, Pan CC, Lin CH, Chu CY, Kung HJ, Cheng CY and Chang PC. REST reduction is essential for hypoxia-induced neuroendocrine differentiation of prostate cancer cells by activating autophagy signaling. Oncotarget 2016; 7: 26137-26151.
[19] Lin YC, Chang YT, Campbell M, Lin TP, Pan CC, Lee HC, Shih JC and Chang PC. MAOA-a novel decision maker of apoptosis and autophagy in hormone refractory neuroendocrine prostate cancer cells. Sci Rep 2017; 7: 46338.
[20] Schoenherr CJ and Anderson DJ. The neuron-restrictive silencer factor (NRSF): a coordinate repressor of multiple neuron-specific genes. Science 1995; 267: 1360-1363.
[21] Liang H, Studach L, Hullinger RL, Xie J and Andrisani OM. Down-regulation of RE-1 silencing transcription factor (REST) in advanced prostate cancer by hypoxia-induced miR-106b~25. Exp Cell Res 2014; 320: 188-199.
[22] Cyrta J, Augspach A, De Filippo MR, Prandi D, Thienger P, Benelli M, Cooley V, Bareja R, Wilkes D, Chae SS, Cavaliere P, Dephoure N, Uldry AC, Lagache SB, Roma L, Cohen S, Jaquet M, Brandt LP, Alshalalfa M, Puca L, Sboner A, Feng F, Wang S, Beltran H, Lotan T, Spahn M, Kruithof-de Julio M, Chen Y, Ballman KV, Demichelis F, Piscuoglio S and Rubin MA. Role of specialized composition of SWI/SNF complexes in prostate cancer lineage plasticity. Nat Commun 2020; 11: 5549.
[23] Chang YT, Lin TP, Tang JT, Campbell M, Luo YL, Lu SY, Yang CP, Cheng TY, Chang CH, Liu TT, Lin CH, Kung HJ, Pan CC and Chang PC. HOTAIR is a REST-regulated lncRNA that promotes neuroendocrine differentiation in castration resistant prostate cancer. Cancer Lett 2018; 433: 43-52.
[24] Chang CH, Cheng TY, Yeh WW, Luo YL, Campbell M, Kuo TC, Shen TW, Hong YC, Tsai CH, Peng YC, Pan CC, Yang MH, Shih JC, Kung HJ, Huang WJ, Chang PC and Lin TP. REST-repressed lncRNA LINC01801 induces neuroendocrine differentiation in prostate cancer via transcriptional activation of autophagy. Am J Cancer Res 2023; 13: 3983-4002.
[25] Mizushima N, Levine B, Cuervo AM and Klionsky DJ. Autophagy fights disease through cellular self-digestion. Nature 2008; 451: 1069-1075.
[26] Hara T, Nakamura K, Matsui M, Yamamoto A, Nakahara Y, Suzuki-Migishima R, Yokoyama M, Mishima K, Saito I, Okano H and Mizushima N. Suppression of basal autophagy in neural cells causes neurodegenerative disease in mice. Nature 2006; 441: 885-889.
[27] Maday S and Holzbaur EL. Autophagosome biogenesis in primary neurons follows an ordered and spatially regulated pathway. Dev Cell 2014; 30: 71-85.
[28] Stavoe AKH and Holzbaur ELF. Autophagy in neurons. Annu Rev Cell Dev Biol 2019; 35: 477-500.
[29] Delk NA and Farach-Carson MC. Interleukin-6: a bone marrow stromal cell paracrine signal that induces neuroendocrine differentiation and modulates autophagy in bone metastatic PCa cells. Autophagy 2012; 8: 650-663.
[30] Derrien T, Johnson R, Bussotti G, Tanzer A, Djebali S, Tilgner H, Guernec G, Martin D, Merkel A, Knowles DG, Lagarde J, Veeravalli L, Ruan X, Ruan Y, Lassmann T, Carninci P, Brown JB, Lipovich L, Gonzalez JM, Thomas M, Davis CA, Shiekhattar R, Gingeras TR, Hubbard TJ, Notredame C, Harrow J and Guigo R. The GENCODE v7 catalog of human long noncoding RNAs: analysis of their gene structure, evolution, and expression. Genome Res 2012; 22: 1775-1789.
[31] Fatica A and Bozzoni I. Long non-coding RNAs: new players in cell differentiation and development. Nat Rev Genet 2014; 15: 7-21.
[32] Gupta RA, Shah N, Wang KC, Kim J, Horlings HM, Wong DJ, Tsai MC, Hung T, Argani P, Rinn JL, Wang Y, Brzoska P, Kong B, Li R, West RB, van de Vijver MJ, Sukumar S and Chang HY. Long non-coding RNA HOTAIR reprograms chromatin state to promote cancer metastasis. Nature 2010; 464: 1071-1076.
[33] Tsai MC, Manor O, Wan Y, Mosammaparast N, Wang JK, Lan F, Shi Y, Segal E and Chang HY. Long noncoding RNA as modular scaffold of histone modification complexes. Science 2010; 329: 689-693.
[34] Wang KC and Chang HY. Molecular mechanisms of long noncoding RNAs. Mol Cell 2011; 43: 904-914.
[35] Schmitt AM and Chang HY. Long noncoding RNAs in cancer pathways. Cancer Cell 2016; 29: 452-463.
[36] Wu W, Gao H, Li X, Zhu Y, Peng S, Yu J, Zhan G, Wang J, Liu N and Guo X. LncRNA TPT1-AS1 promotes tumorigenesis and metastasis in epithelial ovarian cancer by inducing TPT1 expression. Cancer Sci 2019; 110: 1587-1598.
[37] Lin N, Lin JZ, Tanaka Y, Sun P and Zhou X. Identification and validation of a five-lncRNA signature for predicting survival with targeted drug candidates in ovarian cancer. Bioengineered 2021; 12: 3263-3274.
[38] Zhang L, Ye F, Zuo Z, Cao D, Peng Y, Li Z, Huang J and Duan L. Long noncoding RNA TPT1-AS1 promotes the progression and metastasis of

colorectal cancer by upregulating the TPT1-mediated FAK and JAK-STAT3 signalling pathways. Aging (Albany NY) 2021; 13: 3779-3797.

[39] Zhang Y, Sun J, Qi Y, Wang Y, Ding Y, Wang K, Zhou Q, Wang J, Ma F, Zhang J and Guo B. Long non-coding RNA TPT1-AS1 promotes angiogenesis and metastasis of colorectal cancer through TPT1-AS1/NF90/VEGFA signaling pathway. Aging (Albany NY) 2020; 12: 6191-6205.

[40] Cheng C, Liu D, Liu Z, Li M, Wang Y, Sun B, Kong R, Chen H, Wang G, Li L, Hu J, Li Y, Chen H, Zhao Z, Zhang T, Zhu S and Pan S. Positive feedback regulation of lncRNA TPT1-AS1 and ITGB3 promotes cell growth and metastasis in pancreatic cancer. Cancer Sci 2022; 113: 2986-3001.

[41] Tang J, Huang F, Wang H, Cheng F, Pi Y, Zhao J and Li Z. Knockdown of TPT1-AS1 inhibits cell proliferation, cell cycle G1/S transition, and epithelial-mesenchymal transition in gastric cancer. Bosn J Basic Med Sci 2021; 21: 39-46.

[42] Cheng W, Yang F and Ma Y. lncRNA TPT1-AS1 promotes cell migration and invasion in esophageal squamous-cell carcinomas by regulating the miR-26a/HMGA1 axis. Open Med (Wars) 2023; 18: 20220533.

[43] Gao X, Cao Y, Li J, Wang C and He H. LncRNA TPT1-AS1 sponges miR-23a-5p in glioblastoma to promote cancer cell proliferation. Cancer Biother Radiopharm 2021; 36: 549-555.

[44] Hu C, Fang K, Zhang X, Guo Z and Li L. Dyregulation of the lncRNA TPT1-AS1 positively regulates QKI expression and predicts a poor prognosis for patients with breast cancer. Pathol Res Pract 2020; 216: 153216.

[45] Huang Y, Zheng Y, Shao X, Shi L, Li G and Huang P. Long non-coding RNA TPT1-AS1 sensitizes breast cancer cell to paclitaxel and inhibits cell proliferation by miR-3156-5p/caspase 2 axis. Hum Cell 2021; 34: 1244-1254.

[46] Li H, Jin J, Xian J and Wang W. lncRNA TPT1‑AS1 knockdown inhibits liver cancer cell proliferation, migration and invasion. Mol Med Rep 2021; 24: 782.

[47] Wei W, Huang X, Shen X, Lian J, Chen Y, Wang W, Huang J and Zhang B. Overexpression of lncRNA TPT1-AS1 suppresses hepatocellular carcinoma cell proliferation by downregulating CDK2. Crit Rev Eukaryot Gene Expr 2022; 32: 1-9.

[48] Dong B, Miao J, Wang Y, Luo W, Ji Z, Lai H, Zhang M, Cheng X, Wang J, Fang Y, Zhu HH, Chua CW, Fan L, Zhu Y, Pan J, Wang J, Xue W and Gao WQ. Single-cell analysis supports a luminal-neuroendocrine transdifferentiation in human prostate cancer. Commun Biol 2020; 3: 778.

[49] Nguyen HG, Yang JC, Kung HJ, Shi XB, Tilki D, Lara PN Jr, DeVere White RW, Gao AC and Evans CP. Targeting autophagy overcomes Enzalutamide resistance in castration-resistant prostate cancer cells and improves therapeutic response in a xenograft model. Oncogene 2014; 33: 4521-4530.

[50] Adler HL, McCurdy MA, Kattan MW, Timme TL, Scardino PT and Thompson TC. Elevated levels of circulating interleukin-6 and transforming growth factor-beta1 in patients with metastatic prostatic carcinoma. J Urol 1999; 161: 182-187.

[51] Drachenberg DE, Elgamal AA, Rowbotham R, Peterson M and Murphy GP. Circulating levels of interleukin-6 in patients with hormone refractory prostate cancer. Prostate 1999; 41: 127-133.

[52] Wise GJ, Marella VK, Talluri G and Shirazian D. Cytokine variations in patients with hormone treated prostate cancer. J Urol 2000; 164: 722-725.

[53] Ku SY, Rosario S, Wang Y, Mu P, Seshadri M, Goodrich ZW, Goodrich MM, Labbe DP, Gomez EC, Wang J, Long HW, Xu B, Brown M, Loda M, Sawyers CL, Ellis L and Goodrich DW. Rb1 and Trp53 cooperate to suppress prostate cancer lineage plasticity, metastasis, and antiandrogen resistance. Science 2017; 355: 78-83.

[54] Stone L. Prostate cancer: hand in hand - Rb1 and Trp53 cooperate to suppress resistance. Nat Rev Urol 2017; 14: 131.

[55] Ge R, Wang Z, Montironi R, Jiang Z, Cheng M, Santoni M, Huang K, Massari F, Lu X, Cimadamore A, Lopez-Beltran A and Cheng L. Epigenetic modulations and lineage plasticity in advanced prostate cancer. Ann Oncol 2020; 31: 470-479.

[56] Zuccato C, Tartari M, Crotti A, Goffredo D, Valenza M, Conti L, Cataudella T, Leavitt BR, Hayden MR, Timmusk T, Rigamonti D and Cattaneo E. Huntingtin interacts with REST/NRSF to modulate the transcription of NRSE-controlled neuronal genes. Nat Genet 2003; 35: 76-83.

[57] Westbrook TF, Hu G, Ang XL, Mulligan P, Pavlova NN, Liang A, Leng Y, Maehr R, Shi Y, Harper JW and Elledge SJ. SCFbeta-TRCP controls oncogenic transformation and neural differentiation through REST degradation. Nature 2008; 452: 370-374.

[58] Lapuk AV, Wu C, Wyatt AW, McPherson A, McConeghy BJ, Brahmbhatt S, Mo F, Zoubeidi A, Anderson S, Bell RH, Haegert A, Shukin R, Wang Y, Fazli L, Hurtado-Coll A, Jones EC, Hach F, Hormozdiari F, Hajirasouliha I, Boutros PC, Bristow RG, Zhao Y, Marra MA, Fanjul A, Maher CA, Chinnaiyan AM, Rubin MA, Beltran H, Sahinalp SC, Gleave ME, Volik SV and Collins CC.

From sequence to molecular pathology, and a mechanism driving the neuroendocrine phenotype in prostate cancer. J Pathol 2012; 227: 286-297.
[59] Crea F. Neuroendocrine prostate cancer: long noncoding RNAs to treat an incurable cancer - an interview with Dr Francesco Crea. Epigenomics 2019; 11: 1461-1462.
[60] de Kok JB, Verhaegh GW, Roelofs RW, Hessels D, Kiemeney LA, Aalders TW, Swinkels DW and Schalken JA. DD3(PCA3), a very sensitive and specific marker to detect prostate tumors. Cancer Res 2002; 62: 2695-2698.
[61] Lemos AEG, Matos ADR, Ferreira LB and Gimba ERP. The long non-coding RNA PCA3: an update of its functions and clinical applications as a biomarker in prostate cancer. Oncotarget 2019; 10: 6589-6603.
[62] Xie C, Yuan J, Li H, Li M, Zhao G, Bu D, Zhu W, Wu W, Chen R and Zhao Y. NONCODEv4: exploring the world of long non-coding RNA genes. Nucleic Acids Res 2014; 42: D98-103.
[63] Elango R, Vishnubalaji R, Shaath H and Alajez NM. Transcriptional alterations of protein coding and noncoding RNAs in triple negative breast cancer in response to DNA methyltransferases inhibition. Cancer Cell Int 2021; 21: 515.
[64] Jia L, Song Y, Mu L, Li Q, Tang J, Yang Z and Meng W. Long noncoding RNA TPT1-AS1 downregulates the microRNA-770-5p expression to inhibit glioma cell autophagy and promote proliferation through STMN1 upregulation. J Cell Physiol 2020; 235: 3679-3689.
[65] Skoufos G, Kakoulidis P, Tastsoglou S, Zacharopoulou E, Kotsira V, Miliotis M, Mavromati G, Grigoriadis D, Zioga M, Velli A, Koutou I, Karagkouni D, Stavropoulos S, Kardaras FS, Lifousi A, Vavalou E, Ovsepian A, Skoulakis A, Tasoulis SK, Georgakopoulos SV, Plagianakos VP and Hatzigeorgiou AG. TarBase-v9.0 extends experimentally supported miRNA-gene interactions to cell-types and virally encoded miRNAs. Nucleic Acids Res 2024; 52: D304-D310.
[66] Mather RL, Wang Y and Crea F. Is HOTAIR really involved in neuroendocrine prostate cancer differentiation? Epigenomics 2018; 10: 1259-1261.

Table S1. Primer sequences for RT-qPCR used in this study

Gene	Forward primer (5'-3')	Reverse primer (5'-3')
TPT1-AS1	TCCTCCAGTAAATCCCAAGC	GATGGGTATGGCTTTGTCAC
ATG2A	GAGCCTTACAGACCACGAG	GTCAGTGTTATCCAGGTTGAG
EGF	TGATTTGCCCTGACTCTACTC	CCACCACGATGACCTTCTG
MAPK10	TTCTTCCCAAGGCTAGTGTG	TCCACTTGTTTATCGAATCCC
PPM1J	ATGACCACAGCAGGTATACAG	GCGGACATCCCTTCTTCAG
PPP2R2C	GGAGCTTCAACATCGTGGAC	AAGAATGAGCGGTTACTGGG
PPP3CB	CGTCAAAGCTGTCCCTTTCC	GCCATGGATGTCACCACAC
RB1CC1	TGACGTAACTGTATCAGAGGG	ATTTGTATCCGTCCCAGCAC
TGFA	CTGTTCGCTCTGGGTATTGTG	CTGAGTGTGGGAATCTGGG
VPS41	ACTTCTGTCAAGGTGTGCTC	CATTCATTCTCCTGAAAGCCT
WIPI1	GCTTCTCTTTCAACCAGGAC	GGGATTTCATTGCTTCCGT